Plant Cell Rep (2014) 33:1697–1710
DOI 10.1007/s00299-014-1648-x

ORIGINAL PAPER

Identification of autophagy-related genes *ATG4* and *ATG8* from wheat (*Triticum aestivum* L.) and profiling of their expression patterns responding to biotic and abiotic stresses

Dan Pei · Wei Zhang · Hong Sun · Xiaojing Wei · Jieyu Yue · Huazhong Wang

Received: 25 April 2014 / Revised: 9 June 2014 / Accepted: 13 June 2014 / Published online: 5 July 2014

Abstract

Key message **The genes coding for wheat ATG4 and ATG8 were cloned and their roles in autophagy were verified. Implications of ATG4/ATG8 in wheat responses to stresses were suggested by expression profiling.**

Abstract Autophagy-related proteins ATG4 and ATG8 are crucial for autophagy biogenesis. ATG4 processes ATG8 precursor to expose its C-terminal glycine for phosphatidyl ethanolamine (PE) lipidation. ATG8, in the form of ATG8-PE adduct, functions in the organization dynamics of autophagic membranes. Here, we report the identification of two/nine members of the ATG4/ATG8 family from common wheat (*Triticum aestivum* L.). Expression of each wheat *ATG4*/*ATG8* could complement the autophagy activity of yeast *atg4*/*atg8* mutant cells. GFP fusion proteins of ATG8s, especially of ATG8s with innate C-terminal-exposed glycines, localized to punctate autophagic membranes. Both of purified ATG4s could cleave ATG8s in vitro, but they had different activities and different preferences for ATG8 substrates. Two times of transcript accumulation, an early one and a late one, of *ATG4s*/*ATG8s* were detected in the early phases of the *Pm21*- and *Pm3f*-triggered wheat incompatible reactions to the powdery mildew causal fungus *Blumeria graminis* f. sp. *tritici* (*Bgt*), and fluorescence microscopy also revealed a *Bgt*-induced enhanced wheat autophagy level in the *Pm21*-triggered incompatible reaction. Only one time of *Bgt*-induced transcript accumulation of *ATG4s*/*ATG8s*, corresponding to but much higher than the late one in incompatible reactions, was detected in a susceptible line isogenic to the *Pm21* resistance line. These results suggested positive roles of ATG4/ATG8-associated autophagy process in the early stage and possible negative roles in the late stage of wheat immunity response to *Bgt*. In addition, expression of wheat *ATG4s*/*ATG8s* was also found to be upregulated by abiotic stress factors and distinctively regulated by different phytohormones.

Keywords Autophagy · ATG4 · ATG8 · Powdery mildew · *Triticum aestivum* L

Abbreviations

ATG	Autophagy-related gene
PE	Phosphatidyl ethanolamine
EST	Expressed sequence tag
ORF	Open reading frame
GFP	Green fluorescent protein
ET	Ethylene

Communicated by Jeong Sheop Shin.

Electronic supplementary material The online version of this article (doi:10.1007/s00299-014-1648-x) contains supplementary material, which is available to authorized users.

D. Pei · W. Zhang · H. Sun · X. Wei · J. Yue · H. Wang (✉)
School of Life Sciences, Tianjin Normal University, Tianjin Key Laboratory of Animal and Plant Resistance, Tianjin 300387, China
e-mail: skywhz@mail.tjnu.edu.cn

D. Pei
e-mail: 415017319@qq.com

W. Zhang
e-mail: 327156983@qq.com

H. Sun
e-mail: 564829796@qq.com

X. Wei
e-mail: 304888791@qq.com

J. Yue
e-mail: skyyjy@mail.tjnu.edu.cn

SA	Salicylic acid
MeJA	Methyl jasmonate
ABA	Abscisic acid
PEG	Polyethylene glycol
qRT-PCR	Quantitative real-time PCR
TA	Transcript accumulation

Introduction

Autophagy is a degradative process adopted by eukaryotic cells to clean up excessive or damaged cellular structures and macromolecules for recycling of nutrients (Liu and Bassham 2012; Li and Vierstra 2012; Klionsky et al. 2012). In autophagy, batch of cytoplasmic materials are engulfed into double membrane-bound autophagosomes and eventually delivered as inner membrane-enclosed autophagic bodies into the vacuole/lysosome for breakdown. So far, 36 autophagy-related (ATG) proteins have been identified in yeast, among which 17 core ATGs are involved in the biogenesis of autophagosomes (Xie and Klionsky 2007; Reggiori and Klionsky 2013). Two ubiquitin-like proteins, ATG8 and ATG12, and their conjugation systems which are essential for autophagy have been studied in detail (Mizushima et al. 1998; Ohsumi 2001; Reggiori and Klionsky 2013). Newly synthesized ATG8 precursor needs cleavage by the cysteine protease ATG4 to expose a C-terminal glycine residue, whereas ATG12 has an innate C-terminal glycine residue. The conjugation systems begin with the ATP-dependent linkage between the ATG8/ATG12 C-terminal glycine and a conservative cystine in the E1-like protein ATG7. Then, ATG8 and ATG12 are, respectively, transferred to the E2-like protein ATG3 and ATG10. Finally, ATG8 is donated to the lipid phosphatidyl ethanolamine (PE) to form ATG8-PE adduct (ATG8 lipidation); ATG12 is connected with ATG5. ATG12–ATG5 directly associates with ATG16 and forms a large complex through ATG16 oligomerization, which may function as an E3-like enzyme to catalyze the last step of ATG8-PE production (Hanada et al. 2007; Romanov et al. 2012). ATG8 lipidation and its autophagic membrane positioning are crucial for autophagic membrane assembly, extension, closure and fusion with vacuole (Nakatogawa et al. 2007; Xie et al. 2008). Besides processing ATG8 to expose its C-terminal glycine, ATG4 can also deconjugate ATG8-PE to release ATG8 from autophagic membranes, which is an important step facilitating autophagosome maturation and converting it into the fusion-capable form (Nair et al. 2012).

The autophagy process is highly conserved and ATG orthologues retain in fungi, plants and mammals (Bassham 2009; Liu and Bassham 2012). As to plants, large scale identifications have suggested a total of 36 ATG genes in *Arabidopsis* (Doelling et al. 2002; Hanaoka et al. 2002; Yoshimoto et al. 2004; Bassham et al. 2006) and certain numbers in rice (Xia et al. 2011) and maize (Chung et al. 2009). ATG4/ATG8 and other key factors in the two conjugation systems are also essential for plant autophagy (Hanaoka et al. 2002; Ketelaar et al. 2004; Yoshimoto et al. 2004; Yoshimoto 2012). The formation processes of *Arabidopsis* ATG8-PE and ATG12–ATG5·ATG16s complex have been simulated using recombinant proteins in vitro (Fujioka et al. 2008). Preliminary work on the identification of ATG4/ATG8 families has also been reported in crop plants as rice (Su et al. 2006; Xia et al. 2011), corn (Chung et al. 2009) and soybean (Xia et al. 2012).

Autophagy has been suggested to play important roles in plant growth, development and responses to biotic and abiotic stresses including nutrition deficiency, oxidation, osmosis, drought and pathogen infections (Bassham et al. 2006; Hayward and Dinesh-Kumar 2011). So far, few studies on mechanisms and physiological functions of autophagy have been reported in crop plants, especially few in common wheat (*Triticum aestivum* L.) which is one of the most important food crops in the world. Here, for the first time, we report the identification of ATG4 and ATG8 family members from common wheat. Evidences from yeast *atg* mutant complementation, subcellular localization of GFP fusion proteins and in vitro enzyme digestion analysis of ATG8s by ATG4s were provided to demonstrate the essential roles of ATG4s/ATG8s we identified on autophagy biogenesis in wheat. Expression profiles of wheat *ATG4s/ATG8s* in response to the powdery mildew causal fungus *Blumeria graminis* f. sp. *tritici* (*Bgt*), to various abiotic stresses and to exogenously applied phytohormones were also presented in detail. These results provided crucial clues for deciphering the underlying roles of ATG4/ATG8 and their associated autophagy process in wheat responses to severe environmental conditions.

Materials and methods

Plant materials and fungal isolate

Two pairs of wheat near isogenic lines were used in this study. One pair was 92R137/Yangmai 158[7] (carrying the broad-spectrum powdery mildew resistance gene *Pm21*) and its recurrent parent Yangmai 158, and the other pair was Michigan Amber/Chancellor[8] (carrying the isolate-specific powdery mildew resistance gene *Pm3f*) and its recurrent parent Chancellor. The prevalent Chinese *Bgt* isolate E09, which is avirulent to *Pm21* and *Pm3f* but virulent to Yangmai 158 and Chancellor, was maintained

on seedlings of the susceptible cultivar Sumai 3 in a spore-proof greenhouse.

Growth conditions and stress/chemical treatments

Wheat seeds were sown in 9-cm pots filled with a mixture of peat, vermiculite and perlite and grown under a 20 °C, 16-h light/8-h dark regime in a controlled climate chamber. Two-leaf stage seedlings were subject to different treatments. *Bgt* inoculation was conducted by heavily shaking off fresh *Bgt* conidiospores from diseased plants onto experiment seedlings. For treatments of exogenous phytohormones, 2 mM salicylic acid (SA), 1 mM Methyl jasmonate (MeJA), 200 μM Ethylene (ET) generator ethephon or 100 μM abscisic acid (ABA) each in 0.05 % Tween-20 were sprayed onto leaves. Seedlings sprayed with 0.05 % Tween-20 were used as controls. For abiotic treatments, seedlings were transferred to Murashige and Skoog (MS) salt solution for several days and then respectively adding in the MS salt solution of 200 mM NaCl (high salinity stress), 20 % PEG-6000 (drought stress) or by depleting NH_4NO_3 and replacing KNO_3 with KCl (nitrogen deficiency). For low temperature/darkness treatment, seedlings were transferred to a 4 °C refrigerator and kept in darkness. Leaves harvested at defined time points were frozen by liquid nitrogen and then stored at −80 °C.

Gene cloning and sequence analysis

Protein sequences of ATG4/ATG8 family members from *Arabidopsis* (Hanaoka et al. 2002) and rice (Xia et al. 2011) were used as electronic probes for TBLASTN search against the dbEST division of GenBank. Wheat ESTs putatively encoding ATG4/ATG8 were downloaded from the TBLASTN results and assembled into contigs in Vector NTI Advance 11.5. If needed, contigs were electronically extended by searching for new terminal ESTs to cover full-length ORFs. Primers (Table S1) were designed based on the assembled contigs for subsequent amplification of cDNAs by RT-PCR. Total RNA was prepared using Trizol (Invitrogen) from leaves of 92R137/Yangmai 158^7 collected 48 h after inoculation of *Bgt*. Here, pathogen inoculation was used as an inducer for enhanced transcription of ATG genes of interest. Extracted RNA was treated with DNaseI (RNase-free), and used as templates for first-strand cDNA synthesis by Oligo dT primers and the Quantscript RT Kit (Tiangen). Wheat *ATG4*/*ATG8* cDNAs were amplified with the high-fidelity Pfu DNA polymerase. Amplified fragments were A-tailed and cloned into the T-tailed vector pGEM®-T Easy (Promega). Giving that wheat is a hexaploid with three homoeologous subgenomes (AABBDD) and thus different members of a gene family may share identical sequences at primer binding sites, more than 10 recombinant clones from each PCR product were picked to sequencing. The serial number for each wheat ATG4/ATG8 member was assigned according to their relationship with the members of *Arabidopsis* ATG4/ATG8 family (Doelling et al. 2002; Hanaoka et al. 2002). Gene sequences were stored in GenBank.

Conservative domains and motifs were predicted in SMART (http://smart.embl-heidelberg.de). Multiple sequence alignment was performed with ClustalX 2.1. Phylogenetic trees were constructed in Mega 5 by the Neighbor-joining method (bootstrap test with 1,000 replicates). Genomic sequences covering upstream promoter regions were obtained by iterative steps of BLAST searching ($E \leq 10^{-5}$) and assembling in the wheat draft genome database (http://www.cerealsdb.uk.net) using cDNA sequences as the first input. cDNA and genomic sequences were compared by Splign (NCBI) to analyze the exon–intron structures of genomic ORFs. Cis-acting elements in promoter sequences were predicted in the PlantCare website (http://bioinformatics.psb.ugent.be/webtools/plantcare/) with a matrix score ≥5.

Complementation test of yeast *atg* mutants

ORFs of wheat *ATG4s*/*ATG8s* were amplified as *Not*I-*Not*I fragments by primers (Table S1) using the pfu DNA polymerase. PCR fragments were each digested and cloned into the yeast expression vector pFL61 in which constitutive expression of each inserted gene was driven by the yeast phosphoglycerate kinase (PGK) gene promoter. Recombinant vectors were sequenced to prove the correct cDNA insertion direction (initiation codon of cDNA adjacent and downstream to the PGK promoter). Wild-type yeast BY4741 and two mutants, *atg4* (BY4741, atg4Δ:: *kanMX*, *MAT a*; *his3Δ1*; *leu2Δ0*; *met15Δ0*; *ura3Δ0*) and *atg8* (BY4741, atg8Δ:: *kanMX*, *MAT a*; *his3Δ1*; *leu2Δ0*; *met15Δ0*; *ura3Δ0*) were purchased from Open Biosystems (Thermo Scientific). Recombinant vectors were each introduced into yeast *atg8* or *atg4* cells according to the LiAc/SS-DNA/PEG TRAFO protocol (Gietz and Schiestl 2007). Positive transformants were screened on SC-U medium. Yeast autophagy complementation test was performed according to Fujiki et al. (2007). Briefly, Yeast cells were cultured with shaking at 30 °C in SC medium to mid-log phase ($OD_{600} = 1$). Cells were then collected, washed and incubated for another 5 h in nutrient deprivation medium (0.67 % nitrogen base, without glucose, amino acids and ammonium sulfate) to induce autophagy. 1 mM phenylmethylsulfonyl fluoride (PMSF) was added in the medium to accumulate autophagic bodies in the vacuoles. The appearance of autophagic bodies was observed using a differential interference contrast microscope (DM5000B, Leica).

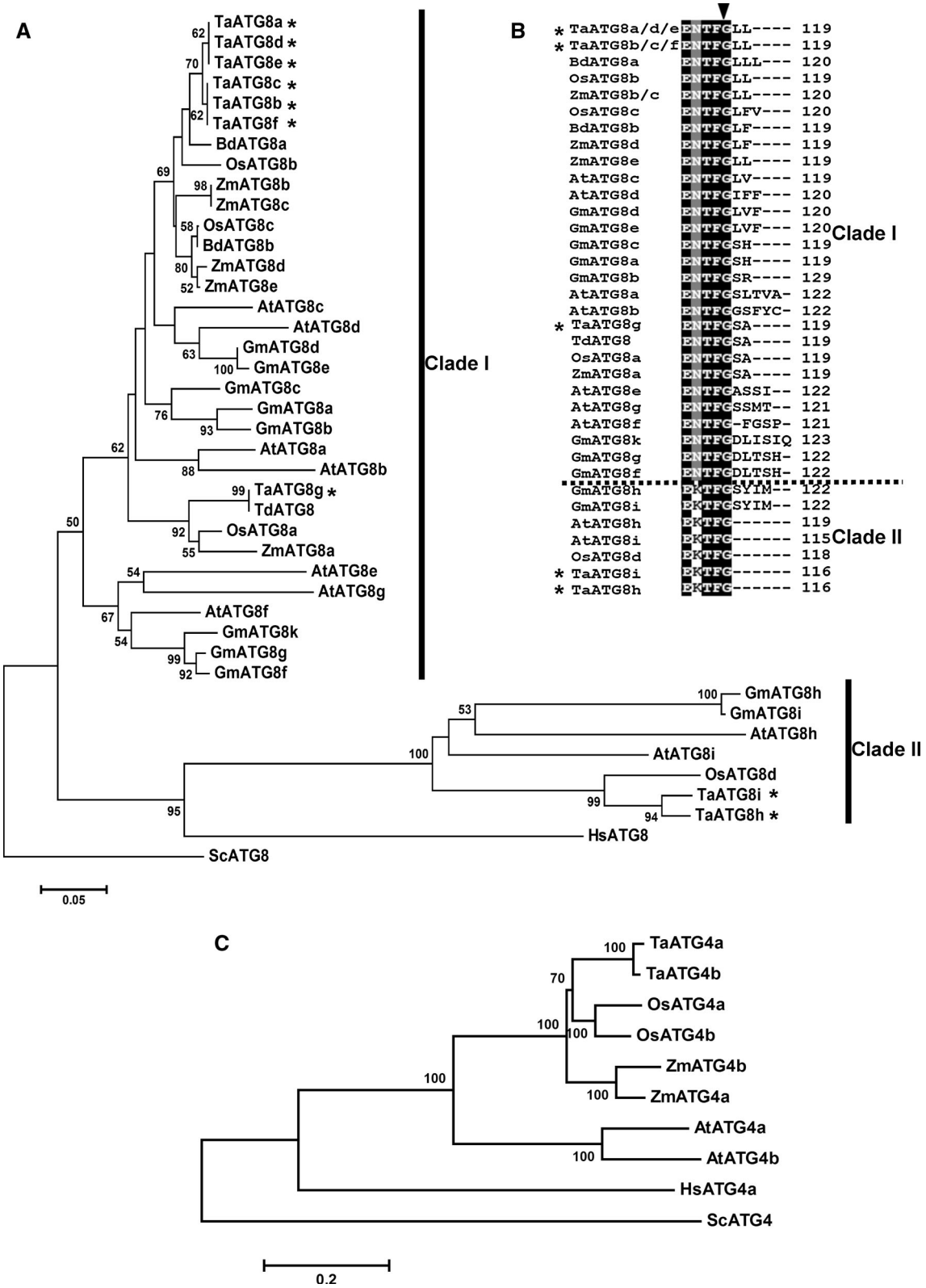
A
TaATG8a *
TaATG8d *
TaATG8e *
TaATG8c *
TaATG8b *
TaATG8f *
BdATG8a
OsATG8b
ZmATG8b
ZmATG8c
OsATG8c
BdATG8b
ZmATG8d
ZmATG8e
AtATG8c
AtATG8d
GmATG8d
GmATG8e
GmATG8c
GmATG8a
GmATG8b
AtATG8a
AtATG8b
TaATG8g *
TdATG8
OsATG8a
ZmATG8a
AtATG8e
AtATG8g
AtATG8f
GmATG8k
GmATG8g
GmATG8f
Clade I
GmATG8h
GmATG8i
AtATG8h
AtATG8i
OsATG8d
TaATG8i *
TaATG8h *
Clade II
HsATG8
ScATG8
0.05
B
* TaATG8a/d/e ENTFGLL---- 119
* TaATG8b/c/f ENTFGLL---- 119
BdATG8a ENTFGLLL--- 120
OsATG8b ENTFGLL---- 119
ZmATG8b/c ENTFGLL---- 120
OsATG8c ENTFGLFV--- 120
BdATG8b ENTFGLF---- 119
ZmATG8d ENTFGLF---- 119
ZmATG8e ENTFGLL---- 119
AtATG8c ENTFGLV---- 119
AtATG8d ENTFGIFF--- 120
GmATG8d ENTFGLVF--- 120
GmATG8e ENTFGLVF--- 120
GmATG8c ENTFGSH---- 119
GmATG8a ENTFGSH---- 119
GmATG8b ENTFGSR---- 129
AtATG8a ENTFGSLTVA- 122
AtATG8b ENTFGGSFYC- 122
* TaATG8g ENTFGSA---- 119
TdATG8 ENTFGSA---- 119
OsATG8a ENTFGSA---- 119
ZmATG8a ENTFGSA---- 119
AtATG8e ENTFGASSI-- 122
AtATG8g ENTFGSSMT-- 121
AtATG8f ENTFG-FGSP- 121
GmATG8k ENTFGDLISIQ 123
GmATG8g ENTFGDLTSH- 122
GmATG8f ENTFGDLTSH- 122
GmATG8h EKTFGSYIM-- 122
GmATG8i EKTFGSYIM-- 122
AtATG8h EKTFG------ 119
AtATG8i EKTFG------ 115
OsATG8d EKTFG------ 118
* TaATG8i EKTFG------ 116
* TaATG8h EKTFG------ 116
Clade I
Clade II
C
TaATG4a
TaATG4b
OsATG4a
OsATG4b
ZmATG4b
ZmATG4a
AtATG4a
AtATG4b
HsATG4a
ScATG4
0.2

◀**Fig. 1** Phylogenetic relationships of eukaryotic ATG4s or ATG8s. Phylogenetic trees were constructed in Mega 5 by the Neighbor-joining method. The reliability of internal branches was assessed by bootstrapping, with 1,000 bootstrap replicates, and values are shown in percentages, with a branching cut-off at 50 %. **a** Phylogenetic tree of eukaryotic ATG8s. **b** Alignment of the C-terminal sequences of plant ATG8s. The conservative glycine residue for PE-conjugation is indicated by an arrowhead. Sequences in **a** and **b** include the nine wheat ATG8s here identified, AER27507 (TdATG8) from *Triticum dicoccoides*, XP_003581707 (BdATG8a) and XP_003571383 (BdATG8b) from *Brachypodium distachyon*, Os07g0512200 (OsATG8a), Os04g0624000 (OsATG8b), Os08g0191600 (OsATG8c) and Os02g0529150 (OsATG8d) from *Oryza sativa*, ACJ73920 (ZmATG8a), ACJ73921 (ZmATG8b), ACJ73922 (ZmATG8c), ACJ73923 (ZmATG8d), and ACJ73925 (ZmATG8e) from *Zea mays*, At4g21980 (AtATG8a), At4g04620 (AtATG8b), At1g62040 (AtATG8c), At2g05630 (AtATG8d), At2G45170 (AtATG8e), At4g16520 (AtATG8f), At3g60640 (AtATG8 g), At3g06420 (AtATG8 h) and At3g15580 (AtATG8i) from *Arabidopsis thaliana*, ACU13796 (GmATG8a), ACU14633 (GmATG8b), ACU17086 (GmATG8c), BAH22449 (GmATG8d), ACU15101 (GmATG8e), ACU19559 (GmATG8f), ACU13862 (GmATG 8 g), ACU16419 (GmATG8 h), BAH22448 (GmATG8i) and ACU19611 (GmATG8 k) from *Glycine max*, NP_009216 (HsATG8, GATE16/GABARAPL2) from Human and NP_009475 (ScATG8) from Yeast. Names of wheat ATG8s are indicated by asterisks. **c** Phylogenetic tree of eukaryotic ATG4s. Sequences in the tree include the two wheat ATG4s here identified, Os03g0391000 (OsATG4a) and Os04g0682000 (OsATG4b) from *Oryza sativa*, ACJ73912 (ZmATG4a) and ACJ73914 (ZmATG4b) from *Zea mays*, At2g44140 (AtATG4a) and At3g59950 (AtATG4b) from *Arabidopsis thaliana*, NP_443168 (HsATG4a) from Human and NP_014176 (ScATG4) from Yeast

Subcellular localization of wheat ATG8s

ORFs of wheat *ATG8s* were amplified using the pfu DNA polymerase by primers with additional restriction sites (Table S1). PCR fragments were each digested and ligated downstream and in-frame with the *GFP* ORF in the vector pA7-GFP, in which expression of each *GFP-ATG8* fusion gene was driven by two tandem-arranged CaMV 35S promoters. Constructed vectors were verified by sequencing. Plasmids were introduced into onion epidermal cells by particle bombardment with PDS1000/He (BioRad) (Scott et al. 1999). GFP fluorescence was visualized by epifluorescence microscopy (DM5000B, Leica) 24 h after bombardment.

In vitro analysis of protease activity of wheat ATG4s on ATG8s

Each of the *Not* I-*Not* I PCR fragments of wheat *ATG4s*/*ATG8s* amplified in the process of yeast expression vector construction was also cloned into the prokaryotic expression vector pET30a. Recombinant vectors were sequenced to prove the correct cDNA insertion direction (initiation codon of cDNA adjacent and downstream to the T7 promoter). Expression vectors were, respectively, transformed into *E. coli* BL21 (DE3) by the heat shock method. Purified recombinant proteins were obtained through 1 mM IPTG-induced expression and Ni affinity chromatography under non-denaturing conditions. In vitro enzyme activity analysis was carried out according to Wu et al. (2012). Briefly, 20 µl reaction buffer (150 mM Nacl, 1 mM EDTA, 1 mM DTT, 50 mM Tris–HCl, pH 7.2) containing purified 0.025 mg mL^{-1} ATG4 and 0.5 mg mL^{-1} ATG8 was kept at 37 °C for 3 h. Then bromophenol blue sample buffer was added to terminate the reaction. Cleaved products were resolved by 15 % SDS-PAGE with 6 M urea in the gel mix to improve resolution.

Expression analysis by quantitative real-time PCR (qRT-PCR)

Gene-specific qRT-PCR primers (Table S1) were designed, and qRT-PCR was conducted in IQ5 (Biorad) using the RealMasterMix (SYBR Green) kit (Tiangen). Each sample was analyzed in triplicate and the experiment was repeated three times. Relative expression level was calculated using the $2^{-\Delta\Delta Ct}$ method (Livak and Schmittgen 2001) with the amplicon of wheat β-tubulin gene as an internal control.

LysoTracker Red staining and microscopy

Wheat leaf segments were infiltrated with 100 µM E-64d (Sigma) and then stained with 2 µM LysoTracker Red DND-99 (Invitrogen) according to the procedure described previously (Liu Y et al. 2005). Florescence was observed under a confocal microscope (ECLIPSE 90i, Nikon) with 543 nm excitation of a 1 mW helium:neon laser with 565–625 nm band pass.

Results

Identification of wheat *ATG8* genes

Plant genomes often contain a plurality of ATG8 paralogs. Likewise, we identified a family of nine ATG8 genes from wheat, eight of which (*TaATG8a–8 h*, GenBank accession KF294807–KF294814) were identified from the cDNA pool of *Bgt*-challenged leaves of the powdery mildew resistant wheat line 92R137/Yangmai 158^{7} and one (*TaATG8i*) by assembly of ESTs (HX189738, CK196170 and HX250137). Nine *TaATG8s* were divided into three subfamilies according to their sequence similarity and evolutionary relationship (Fig. 1a, Fig. S1). The six members (*TaATG8a–8f*) of subfamily I encode only two amino acid sequences (119 A.A.), one by *TaATG8a*, *8d* and *8e* and the other by *TaATG8b*, *8c* and *8f*, with only one residue difference. *TaATG8g*, the sole member of subfamily II,

encodes an amino acid sequence (119 A.A.) with 93 % similarity to members of subfamily I. Wheat *TaATG8g* has identical nucleotide sequence with the reported *ATG8* from *Triticum dicoccoides* (AABB) which is a wheat wild progenitor (Kuzuoglu-Ozturk et al. 2012). There are two members in subfamily III, *TaATG8h* and *8i*, and their nucleotide sequences (351 bp) and encoded amino acid sequences (116 A.A.), respectively, have 96.2 and 97 % identity/similarity. Subfamily III nucleotide/amino acid sequences are 61.5–64.1 %/68 % and 75–76 %/70 % identical/similar to subfamily I and subfamily II, respectively. All of the nine TaATG8s contain an ATG8 ubiquitin domain (pfam: PF02991), within which six essential residues for the N-terminal microtubule binding site, three for the ATG7 binding site and the C-terminal conservative glycine residue for lipidation were predicted (Fig. 1b, Fig. S1).

In the phylogenetic tree, plant ATG8s are clustered into two main clades, Clade I and II (Fig. 1a). Clade I covers the majority of plant ATG8 family members comprising all the members from wheat ATG8 subfamily I and II, 7/9 members from *Arabidopsis*, 3/4 from rice, 8/10 from soybean and 5/5 from maize, which suggests that the ancestor of Clade I and its descents duplicated more frequently within genomes during evolution. However, high similarities were retained in clade I between paralogs (81–100 %) and between orthologues (80–100 %). Clade II covers 1–2 plant ATG8 family members from each species including TaATG8h–8i of wheat subfamily III. Long branches within clade II suggest that the ancestor of Clade II and its descents experienced rapid evolution processes before and after the differentiation of monocots and dicots. The similarity between Clade I and Clade II is 64–71 %. The ancestor of clade II is related to the production of human ATG8. All plant ATG8s hold the C-terminal conservative glycine residue waiting for PE-conjugation (Fig. 1b, Fig. S1). For ATG8s in clade I, the glycine residue is generally protected by additional 2–6 residues and needs ATG4 cleavage to expose, whereas ATG8s in clade II (except ATG8h and 8i of soybean) have post-translationally exposed C-terminal glycine residues.

BLAST searching against the draft genome sequences of the wheat A-genome progenitor *Triticum urartu* (Ling et al. 2013) and the D-genome progenitor *Aegilops tauschii* (Jia et al. 2013) revealed several *ATG8* sites on chromosomes 2AL, 2AS, 2D and 5D. Previously, copies of *T. dicoccoides ATG8* were mapped on chromosomes 1B, 2A and 2D (Kuzuoglu-Ozturk et al. 2012). The genomic ORF sequences of *TaAT8a* and *8g* have similar four-intron structures with a slight difference in intron size (Fig. 2). The genomic ORF sequence of *TaATG8h* also contains four introns, but its introns are greatly extended (the second intron) or shortened (the first and third introns) compared to *TaATG8a* and *8g* (Fig. 2).

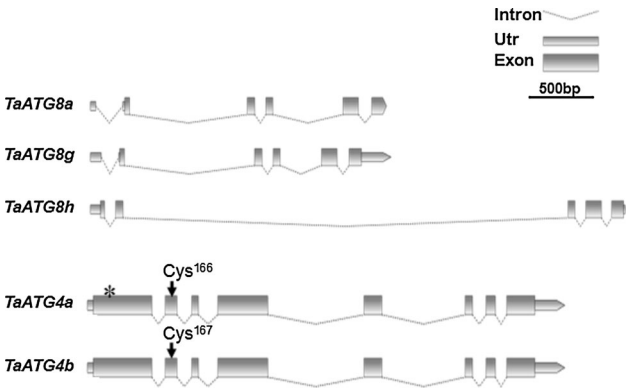

Fig. 2 Diagram models of wheat *ATG4* and *ATG8* genes. An *asterisk* indicates the site in *TaATG4a* where a deletion of three consecutive bases (a codon for alanine) occurs relative to *TaATG4b*; *Arrows* indicate the site encoding the conserved cysteine residue in the catalytic active center of *TaATG4a* and *4b*

Identification of wheat *ATG4* genes

Two wheat ATG4 genes (*TaATG4a–4b*, GenBank accession KF294797–KF294798) were identified from the cDNA pool of *Bgt*-challenged leaves of 92R137/Yangmai 158[7]. *TaATG4a* has an ORF of 1,452 bp encoding a 483 A.A. protein, and *TaATG4b* has an ORF of 1,455 bp encoding a 484 A.A. protein. Three consecutive nucleotides encoding the N-terminus Ala[32] of TaATG4b were deleted in *TaATG4a* (Fig. 2, Fig. S2). The nucleotide and amino acid sequence similarities between TaATG4a and 4b are 96.7 and 97 %, respectively. Both of TaATG4a and 4b have a typical Peptidase_C54 domain (Pfam: PF03416) and a canonical catalytic triad of cysteine protease with three conserved residues: Cys, Asp and His (Fig. S2).

In the phylogenetic tree, ATG4s from different plant species were clustered in separate branches (Fig. 1c), suggesting that ATG4 duplication occurred after the respective speciation of *Arabidopsis*, wheat, rice and maize. For entire sequences, wheat ATG4s share 83–84, 79–80 and 64–67 % similarities with those of rice, maize and *Arabidopsis*, respectively. Wheat ATG4s share only 30–31 and 38–39 % similarities with orthologues of yeast and human, much lower than the corresponding ATG8 s similarities of 72–90 % (between wheat and yeast) and 71–78 % (between wheat and human). The Peptidase_C54 domain sequences are conserved among plant ATG4s and some key residues conserved among all eukaryotic ATG4s (Fig. S2). However, the N-terminal sequences before the Peptidase_C54 domain are much diverged between species, and the human ATG4a has a greatly shortened

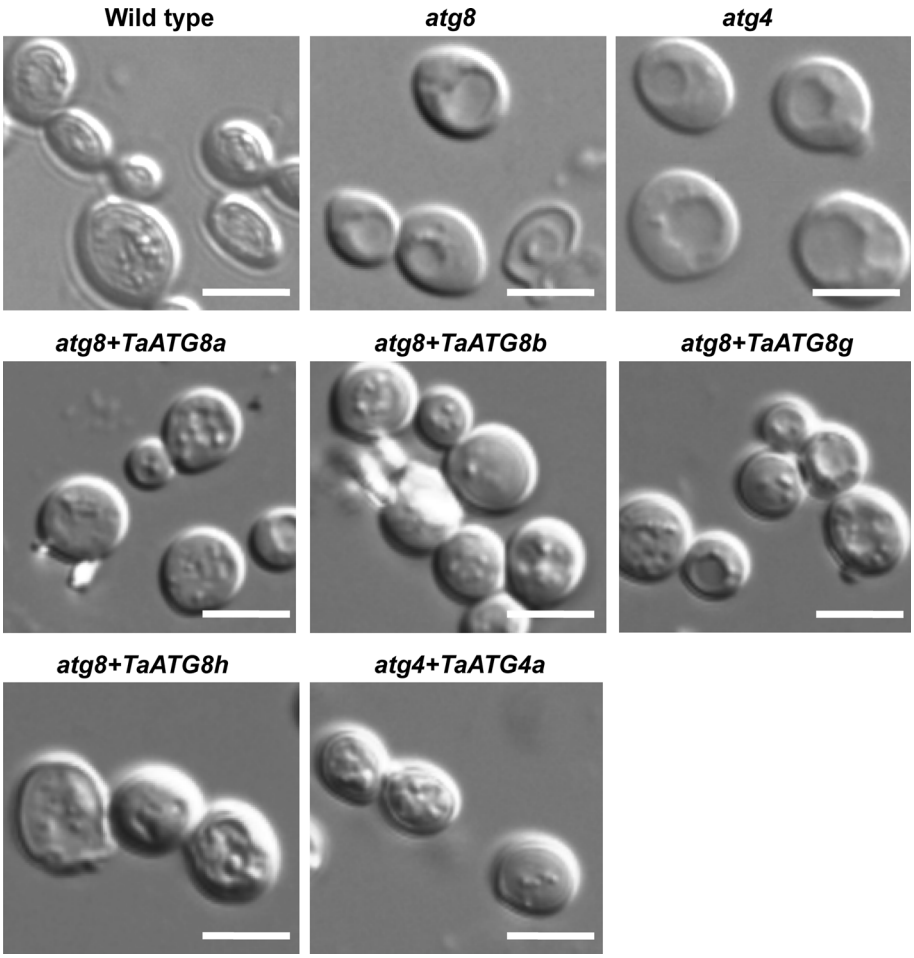

Fig. 3 Functional complementation of *atg4* or *atg8* mutant yeast by wheat *ATG4s* or *ATG8s*. Each wheat *ATG4*/*ATG8* gene was cloned in the plasmid pFL61 and, respectively, expressed in *atg4* or *atg8* yeast cells. Cells grown to mid-log phase were collected, washed, and subsequently incubated for another 5 h in nutrient deprivation medium in the presence of 1 mM PMSF. The appearance of autophagic bodies was observed using a differential interference contrast microscope. *Scale bar* 5 μm

N-terminal sequence. The C-terminal sequences after the Peptidase_C54 domain differ mainly between monocot and dicot ATG4s (Fig. S2).

Results from BLAST searching in the mapped wheat EST database at Graingenes (http://wheat.pw.usda.gov) showed that a homologous EST of *TaATG4* mapped on wheat chromosomes 2AL, 2BL and 2DL. The genomic ORF sequences of *TaATG4a* and *4b* have very similar structures with seven introns (Fig. 2).

Wheat *ATG4s* and *ATG8s* rescue yeast autophagy

Yeast expression vectors were constructed for wheat *ATG4s* and *ATG8s* and introduced, respectively, into yeast *atg4* and *atg8* mutant cells. After 5-h nutrient starvation induction, wild-type yeast (BY4741) cells accumulated numerous autophagic bodies in vacuoles, which were not (*atg8*) or rarely (*atg4*) observed in mutant cells (Fig. 3). Expression of wheat ATG genes partially recovered the autophagy function of yeast *atg8* cells (expressing *TaATG8a*, *8b*, *8g* or *8h*) or *atg4* cells (expressing *TaATG4a*), evidenced by the significantly increased number of autophagic bodies in vacuoles (Fig. 3). Successful complementation verified that wheat TaATG8a, 8b, 8g and 8h are functional homologues of yeast ATG8, and TaATG4a functional homologue of yeast ATG4.

GFP-TaATG8s localize to autophagic membranes

Localization of ATG8 on the surface of autophagic membranes is essential for autophagy biogenesis. TaATG8a and 8b, 8g and 8h, respectively, representing the wheat ATG8 Subfamily I, Subfamily II and Subfamily III, were selected for subcellular localization analysis. Punctate structures were clearly observed in onion epidermal cells expressing GFP-TaATG8h, which may indicate autophagosomes or their immature structures (Fig. 4). Fluorescence of the other three constructs, GFP-TaATG8a, 8b and 8g, showed few punctate structures and sometimes were even diffusely distributed throughout the cell like the fluorescence in cells expressing GFP alone (Fig. 4). Subcellular localization results suggest that the four wheat ATG8s could be recruited to autophagic membranes and thus involved in autophagy biogenesis.

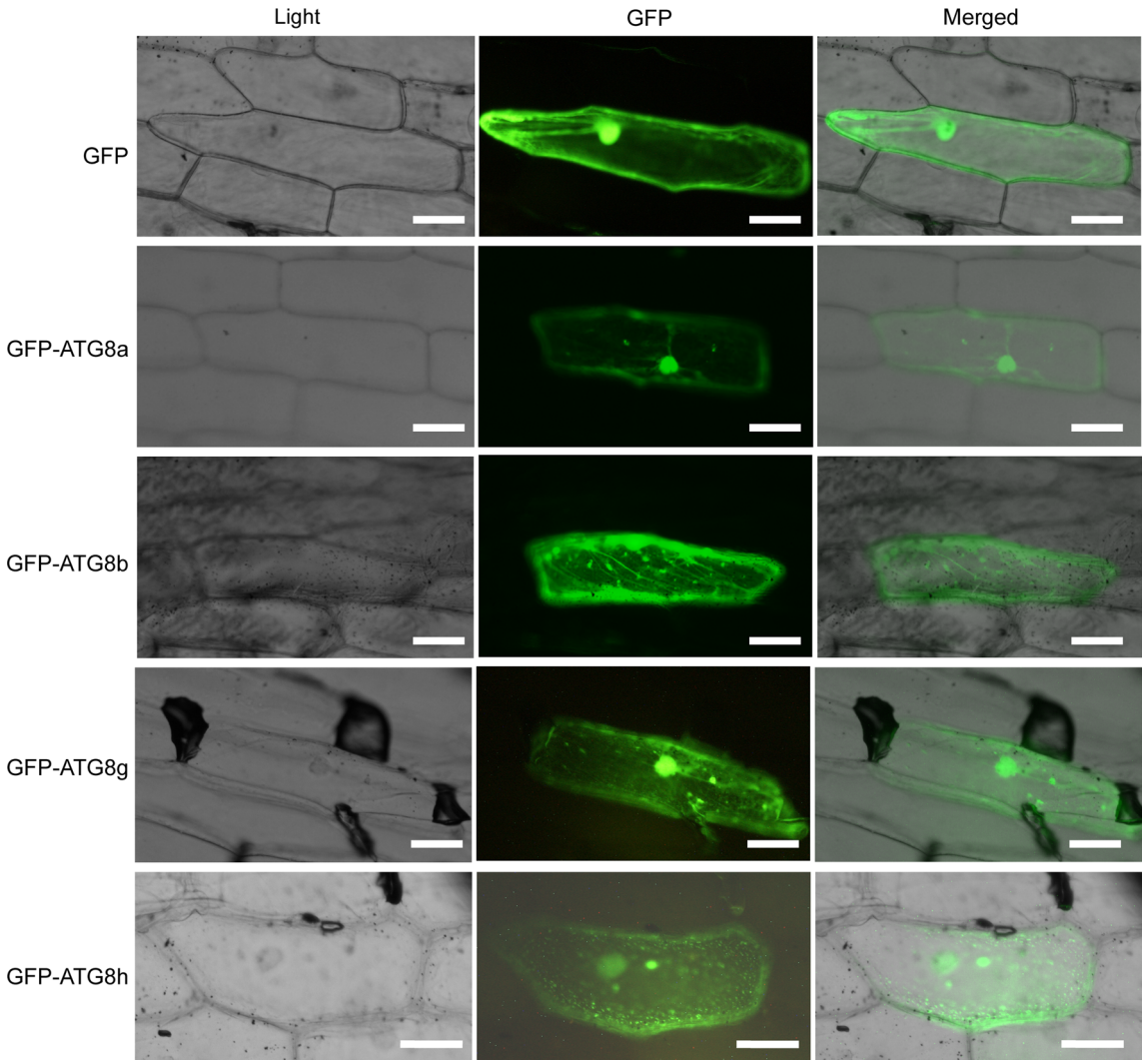

Fig. 4 Subcellular localization of wheat ATG8s in onion epidermal cells. Fluorescence microscopy images of onion epidermal cells transiently expressing either green fluorescent protein (GFP) alone or GFP-TaATG8a, GFP-TaATG8b, GFP-TaATG8g, GFP-TaATG8h fusion proteins. *Scale bar* 50 μm

Wheat ATG4s cleave ATG8s in vitro

ATG8 precursor needs cleavage by the protease ATG4 to expose its N-terminal glycine for PE lipidation. To prove this for wheat ATG4s and ATG8s, purified recombinant proteins of TaATG4a, 4b, 8a, 8b and 8g were obtained through IPTG-induced expression in E. coli and subsequent Ni affinity chromatography. In vitro digestion experiments showed that TaATG8a, 8b, 8g can all be used as cleavage substrates by the two wheat ATG4s (Fig. 5). TaATG4b cleaved the three substrates more efficiently than TaATG4a, and have the highest efficiency towards TaATG8a (Fig. 5).

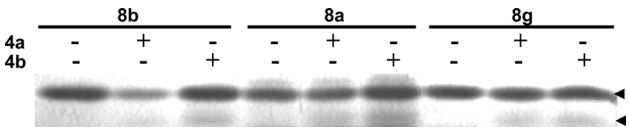

Fig. 5 Wheat ATG8s are cleaved at their C termini by wheat ATG4 proteases. Each wheat *ATG4*/*ATG8* was cloned in the vector pET30a and, respectively, expressed through 1 mM IPTG induction in *E. coli* BL21 (DE3). Purified recombinant proteins were obtained by Ni affinity chromatography under non-denaturing conditions. Protease cleavage analysis was conducted in a 20-μl reaction buffer containing 0.025 mg mL^{-1} TaATG4 and 0.5 mg mL^{-1} TaATG8 at 37 °C for 3 h. Cleaved products were resolved by 15 % SDS-PAGE with 6 M urea in the gel mix to improve resolution. *Arrowheads* indicate the uncleaved forms of ATG8s (*upper bands*) and ATG4s-cleaved forms of ATG8s (*lower bands*), respectively

Expression of wheat *ATG4s* and *ATG8s* positively responds to abiotic stresses

Autophagy has been reported to participate in plant responses to abiotic stresses (Bassham et al. 2006). Thus, we exposed the line Yangmai 158 to several abiotic stresses and characterized the expression profiles of *TaATG4a*, *4b*, *8a*, *8g* and *8h* by qRT-PCR. All these five genes showed upregulated expression upon exposure to high salinity, drought, low temperature/darkness (carbon deficiency imposed by impaired photosynthesis) or nitrogen deficiency (Fig. 6a). Drought treatment resulted in the strongest activation of the five genes and had a prolonged effect on *TaATG4a* and *4b*. Low temperature/darkness treatment upregulated the expression of the three *TaATG8s* more quickly than the other treatments. Among the three *TaATG8s*, *TaATG8a* showed the highest transcript accumulation under the treatment of high salinity, and *TaATG8h* showed the highest transcript accumulation under the treatments of drought and low temperature/darkness, but the lowest transcript accumulation under the treatment of high salinity. As to the two *TaATG4s*, *TaATG4a* showed higher transcript accumulation under the treatments of low temperature/darkness and nitrogen deficiency, and *TaATG4b* showed higher transcript accumulation under the treatment of drought.

Expression of wheat *ATG4s* and *ATG8s* responds to fungus infection

Pathogen infections can induce the expression of plant ATG genes (Hayward and Dinesh-Kumar 2011). To determine if infection by the powdery mildew causal fungus *Bgt* has such effect on wheat, expression of *TaATG4a*, *4b*, *8a*, *8g* and *8h* in *Bgt*-challenged wheat leaves was profiled by qRT-PCR in a time period of 0–36 h after inoculation (hai) of *Bgt*. Two powdery mildew resistance types, *Pm21*-triggered broad-spectrum resistance and *Pm3f*-triggered isolate-specific resistance, and two susceptible wheat genotypes were considered in this analysis.

In the *Pm21*- and *Pm3f*-triggered incompatible reactions (Fig. 6b), the five wheat ATG genes exhibited two *Bgt*-induced transcript accumulation (TA) events, an early one and a late one. The early TAs peaked at 6–10 hai, which is around the time when *Bgt* appressorium germ tubes initially contact and recognize wheat leaf epidermal cells and attempt to invade them. On the contrary to the early TAs in the incompatible reactions, all five genes showed continuous decreased expression during 0–16 hai in the Yangmai 158-*Bgt* compatible reaction, and four of them showed such decreased expression during 0–6 hai in the Chancellor-*Bgt* compatible reaction (Fig. 6b). The late TAs in the two incompatible reactions peaked at 16–24 hai or beyond the last investigation time point of 36 hai. Similarly, this time of TA also occurred in the two compatible reactions (Fig. 6b). Around the period of 16–24 hai is the time when invaded structures of *Bgt* strive in host cells for successful haustorium formation and parasite establishment. The late TAs suggested a second time of ATG4s/ATG8s recruitment occurring after 16 hai in wheat response to *Bgt* infection. In addition, the late TAs of the analyzed genes were much faster and stronger in the susceptible line Yangmai 158 than in the Yangmai 158-isogenic resistance line 92R137/Yangmai 158[7] (Fig. 6b). These *Bgt*-induced expression profiles imply that ATG4s/ATG8s are universally required in wheat broad-spectrum and isolate-specific resistance responses and in susceptible responses to *Bgt*.

Wheat autophagy is induced by *Bgt* infection

Since expression of *TaATG4s*/*TaATG8s* positively responds to *Bgt* infection, we then infiltrated *Bgt*-inoculated leaves with E-64d and stained them with LysoTracker Red to determine if upregulated expression of ATG genes is in line with elevated autophagy level. E-64d is a membrane-permeable cysteine protease inhibitor and has been successfully used in plant to accumulate autophagic bodies inside autolysosomes including vacuoles and small lytic organelles (Inoue et al. 2006; Bassham 2007). LysoTracker Red is dye which labels acidic organelles such as lysosomes and endosomes. This dye also stains autophagosomes/autolysosomes and dotted structures labeled by this dye have widely been recognized as indicative of plant autophagy activity (Moriyasu et al. 2003; Liu Y et al. 2005; Hofius et al. 2009; Lai et al. 2011; Kwon et al. 2013). Before *Bgt* inoculation, LysoTracker Red-stained autolysosome-like structures were rarely observed in leaf epidermal cells of the resistant line 92R137/Yangmai 158[7] (Fig. 7). After *Bgt* inoculation, weak (8 hai) or strong (24 hai) level of punctate autolysosome-like structures were detected (Fig. 7), suggesting an enhanced autophagy level required in the *Pm21*-triggered wheat immune response to *Bgt*. For the susceptible line Yangmai 158, however, LysoTracker Red-stained punctate structures were rarely detected regardless of *Bgt* infection (data not shown). Thinking of the enhanced expression of *TaATG4s*/*TaATG8s* in Yangmai 158 during 16–24 hai, we cannot exclude that autophagy might become activated in this wheat-*Bgt* compatible interaction, but failed to be detected by us.

Expression of wheat *ATG4s* and *ATG8s* responds to exogenously applied phytohormones

Phytohormone signaling pathways are implicated in the involvement of autophagy in plant responses to biotic or abiotic stresses (Liu and Bassham 2012). We hypothesized

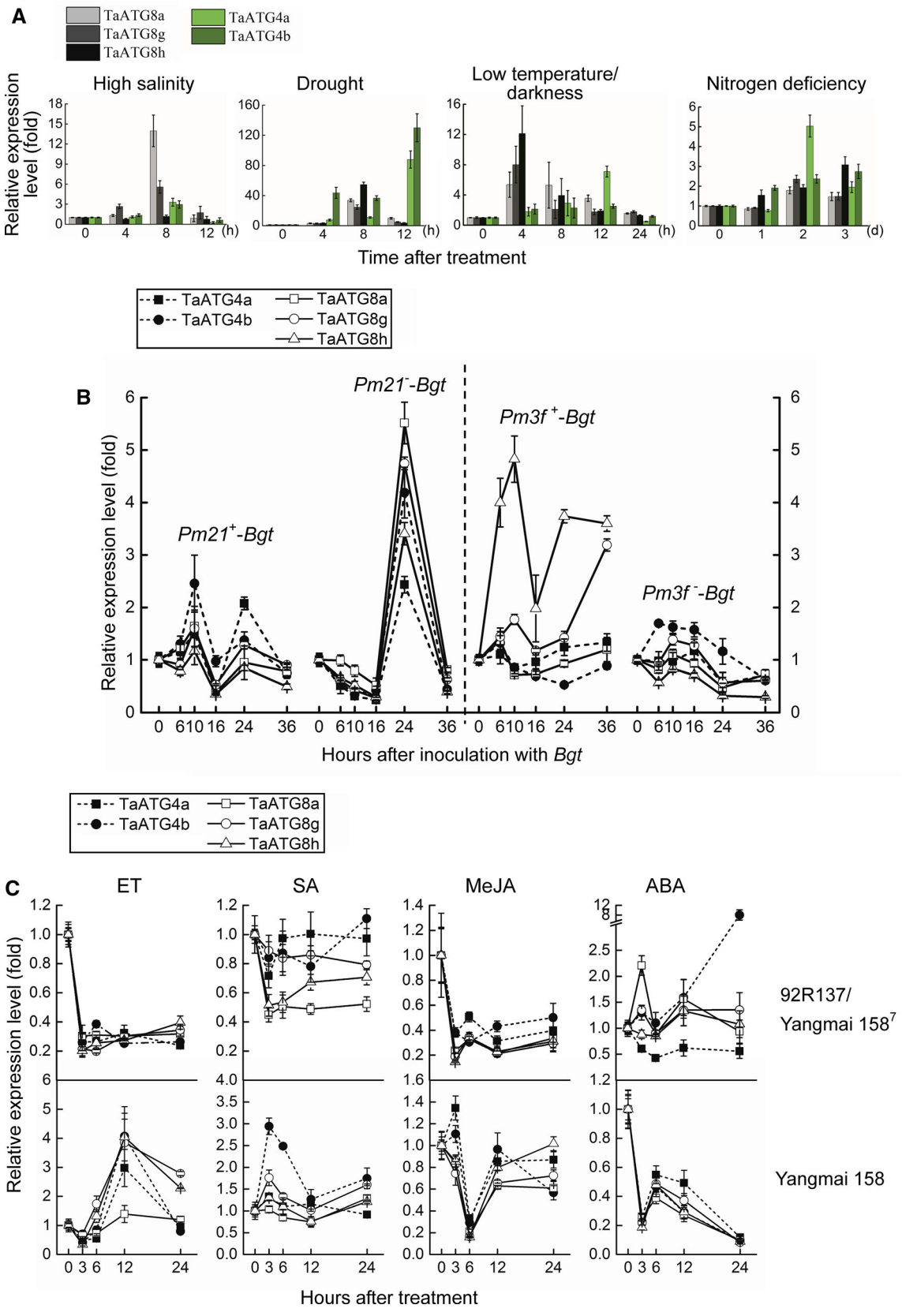
A
TaATG8a
TaATG8g
TaATG8h
TaATG4a
TaATG4b
High salinity
Drought
Low temperature/ darkness
Nitrogen deficiency
Relative expression level (fold)
Time after treatment
B
Pm21-Bgt
Pm21+-Bgt
Pm3f+-Bgt
Pm3f--Bgt
Relative expression level (fold)
Hours after inoculation with Bgt
C
ET
SA
MeJA
ABA
92R137/ Yangmai 158[7]
Yangmai 158
Relative expression level (fold)
Hours after treatment

◀**Fig. 6** Expression patterns of wheat *ATG4s* and *ATG8s*. **a** Expression of wheat *ATG4s* and *ATG8s* in responses to abiotic stresses. **b** Expression of wheat *ATG4s* and *ATG8s* in response to *Bgt* infection. **c** Expression of wheat *ATG4s* and *ATG8s* in responses to phytohormone treatments. Two-leaf stage seedlings were subject to different treatments. For abiotic stress treatments (**a**), Yangmai 158 seedlings cultured in Murashige and Skoog (MS) salt solution were treated by, respectively, adding in the MS salt solution of 200 mM NaCl (high salinity), 20 % PEG-6000 (drought) or by depleting the NH_4NO_3 and replacing the KNO_3 with KCl (nitrogen deficiency). For low temperature/darkness treatment, seedlings were transferred to 4 °C refrigerator and kept in darkness. Pathogen inoculation (**b**) was conducted by heavily shaking off fresh *Bgt* conidiospores from diseased plants onto seedlings of the isogenic lines 92R137/Yangmai 158[7] (*Pm21*$^+$) and Yangmai 158 (*Pm21*$^-$) and the isogenic lines Michigan Amber/Chancellor[8] (*Pm3f*$^+$) and Chancellor (*Pm3f*$^-$). For treatments of exogenous phytohormones **(c)**, 2 mM SA, 1 mM MeJA, 200 μM ethephon (ET generator) or 100 μm ABA each in 0.05 % Tween-20 were sprayed onto leaves of the isogenic lines 92R137/Yangmai 158[7] and Yangmai 158. Samples were collected at the indicated time points after the initiation of treatment. Total RNA was extracted and quantitative real-time PCR (qRT-PCR) analyses were performed with wheat ATG gene-specific primers. The relative expression was normalized by the wheat β-tubulin gene and relative to the control value measured at 0 h. Data represent the average of three independent experiments ± standard deviation (SD, $n = 3$)

that the expression of wheat *ATG4s* and *ATG8s* can be regulated by phytohormones and that the regulating patterns by same phytohormones have some difference between powdery mildew resistance lines and susceptible lines. Expression analysis (Fig. 6c) revealed that ET and SA treatments inhibited the expression of *TaATG4a*, *4b*, *8a*, *8g* and *8h* in the resistance line 92R137/Yangmai 158[7], whereas significantly activated their expression in the susceptible line Yangmai 158. Contrarily, ABA had an activation effect on the resistant line, but an inhibition effect on the susceptible line. MeJA showed inhibitory effects on both of the two lines with a longer duration on the resistance line. For in-depth analysis of the regulation mechanisms of wheat ATG genes in response to pathogen infection and to phytohormone signaling pathways, cis-acting elements were examined on *TaATG4b* and *8a* promoter sequences 2 kb upstream of the predicted transcription start sites. There are three MeJA-response elements (CGTCA motif), one ABA/drought-response element (ABRE) and three defense reaction response elements (one Box-W1, one TC-rich repeats and one CCAAT Box) in the *TaATG4b* promoter. There are two ABA/drought-response elements (ABRE) in the *TaATG8a* promoter. In addition, the *TaATG4b* promoter contains 23 light-response elements, and four tissue-specific expression control elements. The *TaATG8a* promoter contains 11 light-response elements, four tissue-specific expression control elements, two low temperature response elements and one heat-stress response element.

Discussion

Wheat has functional homologues of yeast ATG4 and ATG8 essential for autophagy

In contrast to yeast, which has a single ATG8, higher eukaryotes usually contain a family of ATG8 members. For

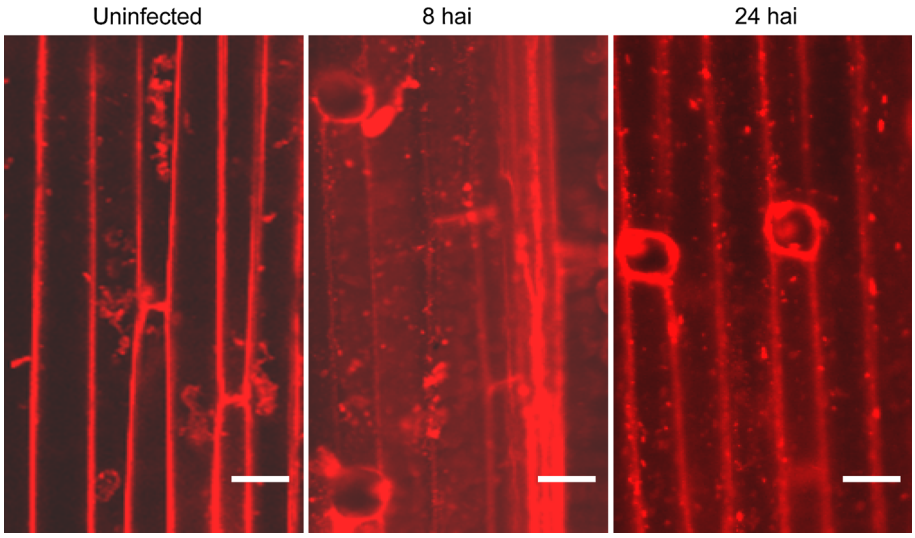

Fig. 7 Autophagy is induced in the *Pm21*-triggered resistance response to *Bgt* infection. Leaf segments of 92R137/Yangmai 158[7] were infiltrated with 100 μM E-64d and then stained with 2 μM LysoTracker Red DND-99. Florescence signals were observed under a confocal microscope (ECLIPSE 90i, Nikon). LysoTracker Red-stained punctate autolysosome-like structures (bright *red spots*) were not observed in leaf epidermal cells of uninfected 92R137/Yangmai 158[7], but weakly at 8 hai and strongly at 24 hai accumulated in leaf epidermal cells of *Bgt*-challenged 92R137/Yangmai 158[7]. Results were reproduced in three independent experiments using three or more plants in each experiment. hai, hours after inoculation of *Bgt* conidiospores. *Scale bar* 50 μm (color figure online)

examples, there are nine ATG8s in *Arabidopsis* (Hanaoka et al. 2002), presumably five in maize (Chung et al. 2009), five in rice (Xia et al. 2011) and 11 in soybean (Xia et al. 2012). Here, we identified nine members of wheat ATG8 family. Since common wheat is a hexaploid species (AABBDD), its ATG8 family may contain more members than we identified. Genes for the six members in subfamily I (*TaATG8a–8f*), for their extreme similarity, may distribute on homoeologous regions of the A, B and D genomes or arise from recent gene duplication events. All wheat ATG8s hold the C-terminal conservative glycine waiting for PE-conjugation. Expanding of the *ATG4* family in wheat genome is not so fast like the *ATG8* family. There are four ATG4s in mammals (Mariño et al. 2003) and a relatively constant number of two in plant species *Arabidopsis* (Hanaoka et al. 2002), rice (Xia et al. 2011) and maize (Chung et al. 2009). In this study, we identified two wheat ATG4s, TaATG4a and 4b, both of which contain a conserved protease activity center.

Successful functional complementation of yeast *atg4* or *atg8* mutants by plant *ATG4* or *ATG8* have been reported in *Arabidopsis* (Ketelaar et al. 2004), soybean (Xia et al. 2012) and *T. dicoccoides* (Kuzuoglu-Ozturk et al. 2012). Here, expression of wheat *TaATG8a*, *8b*, *8g*, *8h* and *4a* also restored autophagy activity in corresponding gene mutant yeast cells. In onion epidermal cells, GFP-TaATG8a, 8b, 8g and 8h showed strong or weak levels of punctate structures, representing autophagosomes and their precursors. *Arabidopsis* GFP-ATG8h/8i with innate C-terminal-exposed glycine appeared in vacuoles more quickly than other GFP-ATG8s (Yoshimoto et al. 2004). Likewise, GFP-TaATG8h with innate C-terminal-exposed glycine exhibited the most obvious punctate distribution. One reason for this situation may be that ATG8s with innate C-terminal-exposed glycine, without the need of ATG4 processing, quickly go through the conjugation reaction cascade and deposit on autophagic membranes, while other ATG8s need an extra step of cleavage by ATG4 which sustains a very limited level under normal conditions (Yoshimoto et al. 2004). In view of the trademark decoration of ATG8-PE on phagophores, extending and mature autophagic membranes and engulfed autophagic bodies in vacuole, observation of GFP-ATG8 puncta has become a routine means for autophagy activity determination (Mitou et al. 2009; Klionsky et al. 2012). Here, we show that GFP-TaATG8h is a potential indicator for determining the dynamics of autophagy in wheat cells. The C-terminal myc-tagged *Arabidopsis* ATG8 recombinant proteins can be cleaved in vitro by ATG4 to remove the tag and protective residues for glycine exposure (Yoshimoto et al. 2004). Our in vitro digestion experiments also showed that both of TaATG4a and 4b can cleave TaATG8a, 8b, and 8g. TaATG4b had a higher efficiency on all the three substrates than TaATG4a, and most efficiently cleaved TaATG8a. Members of ATG4 family from worm and *Arabidopsis* also have different activity and different preference for ATG8 substrates (Wu et al. 2012; Woo et al. 2014). Collectively, we identified wheat ATG4 and ATG8 family members and provide evidences for their involvement in wheat autophagy process.

Expression profiles suggest positive roles of ATG4 and ATG8 in wheat immunity to *Bgt*

The induced expression profiles suggest that TaATG4s and TaATG8s are implicated in wheat responses to abiotic stresses and to infection by the biotrophic pathogen fungus *Bgt*. Two TA events of *TaATG4s* and *TaATG8s* chronologically occurred in the *Pm21*- and *Pm3f*-triggered wheat incompatible reactions to *Bgt* during 0–36 hai. The late TAs of analyzed genes were also detected in the compatible reactions, but the former early TAs in the incompatible reactions formed a sharp contrast to the downregulation patterns in the compatible reactions. These two *Bgt*-induced TA events, especially the early one, implied that wheat ATG4s and ATG8s are employed in the early stage of wheat resistance response to *Bgt*. Pathogen-induced expression of plant ATG genes is consistent with enhanced autophagy levels (Liu Y et al. 2005; Patel and Dinesh-Kumar 2008). Likewise, accumulation of LysoTracker Red-stained autolysosome-like structures was detected in *Bgt*-challenged leaf epidermal cells of the resistance line 92R137/Yangmai 158[7], which links the effects of ATG4 s/ATG8 s on wheat immunity to *Bgt* with their associated cellular process, autophagy. A positive role of autophagy on plant immunity has been reported in plant-pathogen systems as *Nicotiana benthamiana* (N)-TMV (incompatible interaction) (Liu Y et al. 2005), *Arabidopsis-Pseudomonas syringae* (compatible interaction) (Patel and Dinesh-Kumar 2008; Hofius et al. 2009), *Arabidopsis-Botrytis cinerea/Alternaria brassicicola* (compatible interactions) (Lenz et al. 2011; Lai et al. 2011) and *Arabidopsis-Sclerotinia sclerotiorum* (incompatible interaction) (Kabbage et al. 2013). Two *Bgt*-induced TA events have been found for many wheat resistance-related genes in wheat resistance responses, which also match the two pathogen-induced oxygen burst processes (Hückelhoven and Kogel 2003; Liu GS et al. 2005). ROS (reactive oxygen species) and cellular redox state may play key roles on autophagy regulation, and autophagy in turn negatively controls the production of ROS induced by pathogen infection (Yoshimoto et al. 2009; Pérez-Pérez et al. 2012).

Expression of *TaATG4s*/*TaATG8s* can be regulated by exogenously applied phytohormones. The ET, SA or ABA-regulated expression patterns were different and even contrast between powdery mildew resistant lines and

susceptible lines. These differences may also occur responding to endogenous phytohormone signaling pathways triggered in wheat response to *Bgt*, and thus contribute to the different *Bgt*-induced levels of TaATG4s/TaATG8s between resistance and susceptible lines.

Wheat ATG4 and ATG8 may also contribute to the pathogenicity of *Bgt*

Much higher levels of enhanced expression were detected for *TaATG4s*/*TaATG8s* in the Yangmai 158-*Bgt* compatible reaction at the late stage around 16–36 hai. Since more *Bgt* conidiospores should have successfully penetrated into host cells of susceptible lines after 16 hai, there is a possibility that the high accumulation levels of TaATG4s/TaATG8s after 16 hai in susceptible lines are accepted and their associated autophagy process hijacked by *Bgt* to help with its pathogenicity including assimilation of nutrients from host cells. Thus, at least in the genetic background of Yangmai 158, ATG4s/ATG8s and probably their associated autophagy process may play a negative role on wheat immunity to *Bgt* after 16 hai. Negative roles of autophagy in plant immunity have been reported on plant-(semi-)biotrophic pathogen systems as *Arabidopsis-P. syringae* and *Arabidopsis*-powdery mildew fungus *Golovinomyces cichoracearum* (Lenz et al. 2011; Wang et al. 2011).

Acknowledgments This work was supported by the Natural Science Foundation of Tianjin, China (Grant number 12JCZDJC23000); the Fok Ying-Tong Education Foundation for Young Teachers in the Higher Education Institutions of China (Grant number 131026); and the Open Fund of Tianjin Key Laboratory of Animal and Plant Resistance, Tianjin Normal University (Grant number 52LX12).

Conflict of interest The authors do not have any conflict of interest.

References

Bassham DC (2007) Plant autophagy-more than a starvation response. Curr Opin Plant Biol 10:587–593

Bassham DC (2009) Function and regulation of macroautophagy in plants. Biochim Biophys Acta 9:1397–1403

Bassham DC, Laporte M, Marty F, Moriyasu Y, Ohsumi Y, Olsen LJ, Yoshimoto K (2006) Autophagy in development and stress responses of plants. Autophagy 2:2–11

Chung T, Suttangkakul A, Vierstra RD (2009) The ATG autophagic conjugation system in maize: *ATG* transcripts and abundance of the ATG8-lipid adduct are regulated by development and nutrient availability. Plant Physiol 149:220–234

Doelling JH, Walker JM, Friedman EM, Thompson AR, Vierstra RD (2002) The APG8/12-activating enzyme APG7 is required for proper nutrient recycling and senescence in *Arabidopsis thaliana*. J Biol Chem 277:33105–33114

Fujiki Y, Yoshimoto K, Ohsumi Y (2007) An *Arabidopsis* homolog of yeast ATG6/VPS30 is essential for pollen germination. Plant Physiol 143:1132–1139

Fujioka Y, Noda NN, Fujii K, Yoshimoto K, Ohsumi Y, Inagaki F (2008) In vitro reconstitution of plant Atg8 and Atg12 conjugation systems essential for autophagy. J Biol Chem 283:1921–1928

Gietz RD, Schiestl RH (2007) Quick and easy yeast transformation using the LiAc/SS carrier DNA/PEG method. Nat Protoc 2:35–37

Hanada T, Noda NN, Satomi Y, Ichimura Y, Fujioka Y, Takao T et al (2007) The Atg12-Atg5 conjugate has a novel E3-like activity for protein lipidation in autophagy. J Biol Chem 282: 37298–37302

Hanaoka H, Noda T, Shirano Y, Kato T, Hayashi H, Shibata D et al (2002) Leaf senescence and starvation induced chlorosis are accelerated by the disruption of an *Arabidopsis* autophagy gene. Plant Physiol 129:1181–1193

Hayward AP, Dinesh-Kumar SP (2011) What can plant autophagy do for an innate immune response? Annu Rev Phytopathol 49:557–576

Hofius D, Schultz-Larsen T, Joensen J, Tsitsigiannis DI, Petersen NH, Mattsson O et al (2009) Autophagic components contribute to hypersensitive cell death in *Arabidopsis*. Cell 137:773–783

Hückelhoven R, Kogel KH (2003) Reactive oxygen intermediates in plant-microbe interactions: who is who in powdery mildew resistance? Planta 216:891–902

Inoue Y, Suzuki T, Hattori M, Yoshimoto K, Ohsumi Y, Moriyasu Y (2006) *AtATG* genes, homologs of yeast autophagy genes, are involved in constitutive autophagy in *Arabidopsis* root tip cells. Plant Cell Physiol 47:1641–1652

Jia J, Zhao S, Kong X, Li Y, Zhao G, He W et al (2013) *Aegilops tauschii* draft genome sequence reveals a gene repertoire for wheat adaptation. Nature 496:91–95

Kabbage M, Williams B, Dickman MB (2013) Cell death control: the interplay of apoptosis and autophagy in the pathogenicity of *Sclerotinia sclerotiorum*. PLoS Pathog 9:e1003287

Ketelaar T, Voss C, Dimmock SA, Thumm M, Hussey PJ (2004) *Arabidopsis* homologues of the autophagy protein Atg8 are a novel family of microtubule binding proteins. FEBS Lett 567:302–306

Klionsky DJ, Abdalla FC, Abeliovich H, Abraham RT, Acevedo-Arozena A, Adeli K et al (2012) Guidelines for the use and interpretation of assays for monitoring autophagy. Autophagy 8:445–544

Kuzuoglu-Ozturk D, Cebeci Yalcinkaya O, Akpinar BA, Mitou G, Korkmaz G, Gozuacik D, Budak H (2012) Autophagy-related gene, TdAtg8, in wild emmer wheat plays a role in drought and osmotic stress response. Planta 236:1081–1092

Kwon SI, Cho HJ, Kim SR, Park OK (2013) The Rab GTPase RabG3b positively regulates autophagy and immunity-associated hypersensitive cell death in *Arabidopsis*. Plant Physiol 161:1722–1736

Lai Z, Wang F, Zheng Z, Fan B, Chen Z (2011) A critical role of autophagy in plant resistance to necrotrophic fungal pathogens. Plant J 66:953–968

Lenz HD, Haller E, Melzer E, Kober K, Wurster K, Stahl M et al (2011) Autophagy differentially controls plant basal immunity to biotrophic and necrotrophic pathogens. Plant J 66:818–830

Li F, Vierstra RD (2012) Autophagy: a multifaceted intracellular system for bulk and selective recycling. Trends Plant Sci 17:526–537

Ling HQ, Zhao S, Liu D, Wang J, Sun H, Zhang C et al (2013) Draft genome of the wheat A-genome progenitor *Triticum urartu*. Nature 496:87–90

Liu Y, Bassham DC (2012) Autophagy: pathways for self-eating in plant cells. Annu Rev Plant Biol 63:215–237

Liu GS, Sheng XY, Greenshields DL, Ogieglo A, Kaminskyj S, Selvaraj G, Wei YD (2005) Profiling of wheat class III

peroxidase genes derived from powdery mildew-attacked epidermis reveals distinct sequence-associated expression patterns. Mol Plant Microbe Interact 18:730–741

Liu Y, Schiff M, Czymmek K, Tallóczy Z, Levine B, Dinesh-Kumar SP (2005) Autophagy regulates programmed cell death during the plant innate immune response. Cell 121:567–577

Livak KJ, Schmittgen TD (2001) Analysis of relative gene expression data using real-time quantitative PCR and the $2^{-\Delta\Delta CT}$ Method. Methods 25:402–408

Mariño G, Uría JA, Puente XS, Quesada V, Bordallo J, López-Otín C (2003) Human autophagins, a family of cysteine proteinases potentially implicated in cell degradation by autophagy. J Biol Chem 278:3671–3678

Mitou G, Budak H, Gozuacik D (2009) Techniques to study autophagy in plants. Int J Plant Genomics 2009:451357

Mizushima N, Noda T, Yoshimori T, Tanaka Y, Ishii T, George MD et al (1998) A protein conjugation system essential for autophagy. Nature 395:395–398

Moriyasu Y, Hattori M, Jauh G, Rogers JC (2003) Alpha tonoplast intrinsic protein is specifically associated with vacuole membrane involved in an autophagic process. Plant Cell Physiol 44:795–802

Nair U, Yen WL, Mari M, Cao Y, Xie Z, Baba M et al (2012) A role for Atg8-PE deconjugation in autophagosome biogenesis. Autophagy 8:780–793

Nakatogawa H, Ichimura Y, Ohsumi Y (2007) Atg8, a ubiquitin-like protein required for autophagosome formation, mediates membrane tethering and hemifusion. Cell 130:165–178

Ohsumi Y (2001) Molecular dissection of autophagy: two ubiquitin-like systems. Nat Rev Mol Cell Biol 2:211–216

Patel S, Dinesh-Kumar SP (2008) Arabidopsis ATG6 is required to limit the pathogen-associated cell death response. Autophagy 4:20–27

Pérez-Pérez ME, Lemaire SD, Crespo JL (2012) Reactive oxygen species and autophagy in plants and algae. Plant Physiol 160:156–164

Reggiori F, Klionsky DJ (2013) Autophagic processes in Yeast: mechanism, machinery and regulation. Genetics 194:341–361

Romanov J, Walczak M, Ibiricu I, Schüchner S, Ogris E, Kraft C, Martens S (2012) Mechanism and functions of membrane binding by the Atg5-Atg12/Atg16 complex during autophagosome formation. EMBO J 31:4304–4317

Scott A, Wyatt S, Tsou PL, Robertson D, Allen NS (1999) Model system for plant cell biology: GFP imaging in living onion epidermal cells. Biotechniques 26(1125):1128–1132

Su W, Ma H, Liu C, Wu J, Yang J (2006) Identification and characterization of two rice autophagy associated genes, *OsAtg8* and *OsAtg4*. Mol Biol Rep 33:273–278

Wang Y, Nishimura MT, Zhao T, Tang D (2011) ATG2, an autophagy-related protein, negatively affects powdery mildew resistance and mildew-induced cell death in *Arabidopsis*. Plant J 68:74–87

Woo J, Park E, Dinesh-Kumar SP (2014) Differential processing of *Arabidopsis* ubiquitin-like Atg8 autophagy proteins by Atg4 cysteine proteases. Proc Natl Acad Sci USA 111:863–868

Wu F, Li Y, Wang F, Noda NN, Zhang H (2012) Differential function of the two Atg4 homologues in the aggrephagy pathway in *Caenorhabditis elegans*. J Biol Chem 287:29457–29467

Xia K, Liu T, Ouyang J, Wang R, Fan T, Zhang M (2011) Genome-wide identification, classification, and expression analysis of autophagy-associated gene homologues in rice (*Oryza sativa* L.). DNA Res 18:363–377

Xia T, Xiao D, Liu D, Chai W, Gong Q, Wang NN (2012) Heterologous expression of ATG8c from Soybean Confers Tolerance to Nitrogen Deficiency and Increases Yield in *Arabidopsis*. PLoS one 7:e37217

Xie Z, Klionsky DJ (2007) Autophagosome formation: core machinery and adaptations. Nat Cell Biol 9:1102–1109

Xie Z, Nair U, Klionsky DJ (2008) Atg8 controls phagophore expansion during autophagosome formation. Mol Biol Cell 19:3290–3298

Yoshimoto K (2012) Beginning to understand autophagy, an intracellular self-degradation system in plants. Plant Cell Physiol 53:1355–1365

Yoshimoto K, Hanaoka H, Sato S, Kato T, Tabata S, Noda T, Ohsumi Y (2004) Processing of ATG8 s, ubiquitin-Like Proteins, and their deconjugation by ATG4 s are essential for plant autophagy. Plant Cell 16:2967–2983

Yoshimoto K, Jikumaru Y, Kamiya Y, Kusano M, Consonni C, Panstruga R et al (2009) Autophagy negatively regulates cell death by controlling *NPR1*-dependent salicylic acid signaling during senescence and the innate immune response in *Arabidopsis*. Plant Cell 21:2914–2927